11

Coulomb Scattering from Extended Charges

We have seen in the preceding chapters that the theory works accurately for phase shift functions of the sort considered in hadron–nucleus scattering problems. It was also shown in chapter 4 that the asymptotic approach gives an exact result for the Coulomb scattering from a point charge. In the present chapter we shall demonstrate that the method retains its accuracy and presents great practical simplifications in problems involving pure Coulomb scattering by charge distributions. In the next chapter, we will consider combinations of such Coulomb interactions with short-range (nuclear) interactions.

Because of the long range of the Coulomb field, numerical evaluation of the diffraction integral, when charges are present, often requires some special treatment. We shall show, however, that in the asymptotic approach, the infinite range of the Coulomb field needn't pose any problem.

Let us first consider scattering from a distributed charge. For a point-like projectile of charge $Z_1 e$, the Coulomb potential is given in terms of the charge density $\rho_{\mathrm{C}}(\boldsymbol{r})$ as

$$V_{\mathrm{C}}(\boldsymbol{r}) = \frac{Z_1 Z_2 e^2}{4\pi} \int \mathrm{d}^3 r' \, \frac{\rho_{\mathrm{C}}(\boldsymbol{r}')}{|\boldsymbol{r} - \boldsymbol{r}'|}, \tag{11.1}$$

where $\int \mathrm{d}^3 r' \rho_{\mathrm{C}}(\boldsymbol{r}') = 1$. The Coulomb phase shift function is then defined as

$$\chi_{\mathrm{C}}(\boldsymbol{b}) = -\frac{1}{\hbar v} \int_{-\infty}^{\infty} \mathrm{d}z \, V_{\mathrm{C}}(\boldsymbol{b}, z). \tag{11.2}$$

The unscreened point charge would actually yield a divergent phase shift function. However, a $\boldsymbol{b}$-independent contribution to the phase shift function by the screening charge, however distant it may be, cancels the divergence, leaving only a finite phase attached to the scattering amplitude. This phase, in practice, depends on atomic parameters, and is usually left unmeasured.

Downloaded from https://www.cambridge.org/core. UNIVERSIDAD AUTONOMA METROPOLITANA, on 19 Nov 2026 at 05:49:58, subject to the Cambridge Core terms of use, available at https://www.cambridge.org/core/terms. https://doi.org/10.1017/9781316219256.015

11.1 Screened Charge Distribution—An Example

We consider the screened charge distribution

$$\begin{aligned}\rho_{\mathrm{C}}(\boldsymbol{r}) &= \rho_+(r) - \rho_-(r), \\ &= \frac{3}{4\pi R_+^3}\theta(R_+ - r) - \frac{1}{4\pi R_-^2}\delta(r - R_-),\end{aligned} \tag{11.3}$$

with $R_+ < R_-$, and where the positive and negative charge distributions are separately normalized, $\int \mathrm{d}^3 r \rho_+(r) = \int \mathrm{d}^3 r \rho_-(r) = 1$. Hence, the total charge is zero. With

$$\int \mathrm{d}\Omega \frac{1}{|\boldsymbol{r} - \boldsymbol{r}'|} = \frac{4\pi}{\max(r, r')}, \tag{11.4}$$

the potential Eq. (11.1) becomes

$$\begin{aligned}V_{\mathrm{C}}(\boldsymbol{r}) &= Z_1 Z_2 e^2 \left[\frac{1}{r}\int_0^r \mathrm{d}r' r'^2 [\rho_+(r') - \rho_-(r')] + \int_r^\infty \mathrm{d}r' r' [\rho_+(r') - \rho_-(r')]\right] \\ &= \frac{Z_1 Z_2 e^2}{4\pi} \begin{cases} \dfrac{3}{2R_+} - \dfrac{r^2}{2R_+^3} - \dfrac{1}{R_-}, & r < R_+ < R_-, \\ \dfrac{1}{r} - \dfrac{1}{R_-}, & R_+ < r < R_-, \\ 0, & R_+ < R_- < r. \end{cases}\end{aligned} \tag{11.5}$$

In Fig. 11.1(a) we show the charge distributions Eq. (11.3) and the resulting potential Eq. (11.5) for $R_+ = 1$, $R_- = 5$ (arbitrary units) and $Z_1 Z_2 e^2 = 4\pi$.

The Coulomb phase shift function can be expressed directly in terms of the potential, by Eq. (11.2), using the integral

$$\int_{z_0}^{z_1} \frac{\mathrm{d}z}{\sqrt{b^2 + z^2}} = \log \frac{z_1 + \sqrt{b^2 + z_1^2}}{z_0 + \sqrt{b^2 + z_0^2}}, \tag{11.6}$$

or, alternatively (see Section 11.2), via the charge thickness function

$$T_{\mathrm{C}}(b) = \int_{-\infty}^{\infty} \rho_{\mathrm{C}}\left(\sqrt{b^2 + z^2}\right) \mathrm{d}z, \qquad 2\pi \int_0^\infty T_{\mathrm{C}}(b) b \, \mathrm{d}b = 1. \tag{11.7}$$

For the screened charge distribution considered, this thickness function is given by

$$T_{\mathrm{C}}(b) = T_{\mathrm{C}}^+(b) - T_{\mathrm{C}}^-(b), \tag{11.8}$$

Downloaded from https://www.cambridge.org/core. UNIVERSIDAD AUTONOMA METROPOLITANA, on 19 Nov 2026 at 05:49:58, subject to the Cambridge Core terms of use, available at https://www.cambridge.org/core/terms. https://doi.org/10.1017/9781316219256.015

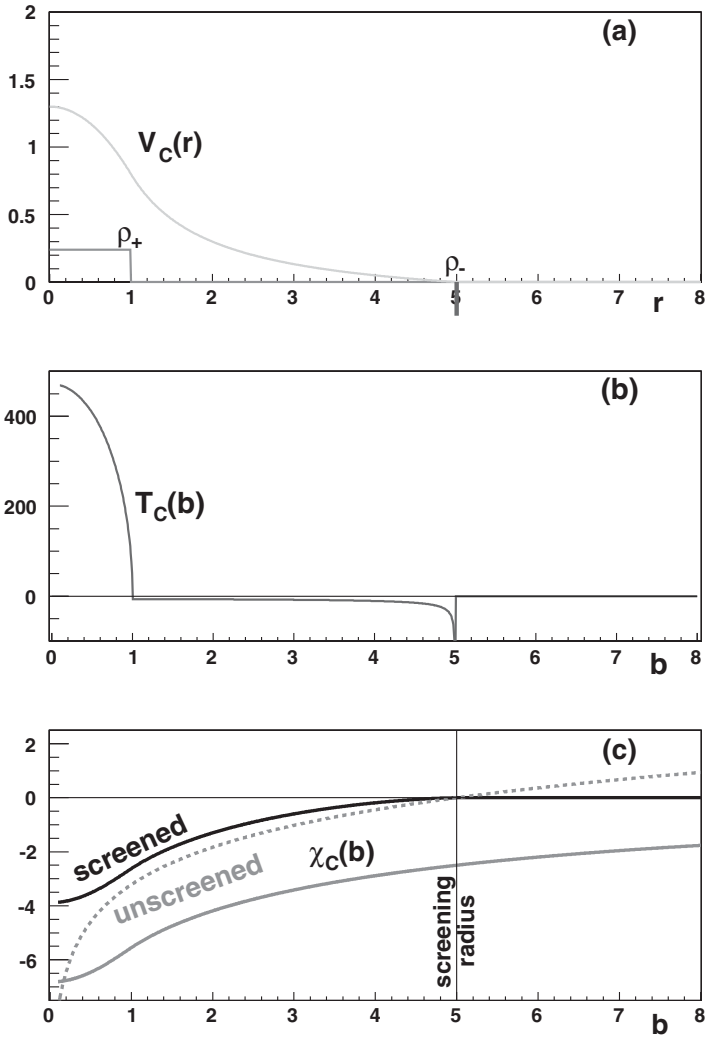


Figure 11.1 Studies of the screened charge distribution defined by Eqs. (11.3), (11.5) and (11.7). (a) Charge distributions ρ_+ and ρ_- (the negative δ-function at $R_- = 5$ is represented by a thick slab) and resulting potential, $V_C(r)$. (b) Thickness function $T_C(b)$. (c) Coulomb phase shift functions: solid: with screening and for finite charge distribution, unscreened (as labeled); dashed: point charge, unscreened.

with

$$T_C^+(b) = \frac{6}{4\pi R_+^2}\sqrt{1-(b/R_+)^2}\,\theta(R_+ - b),$$
$$T_C^-(b) = \frac{2}{4\pi R_-^2}\frac{1}{\sqrt{1-(b/R_-)^2}}\,\theta(R_- - b) \qquad (11.9)$$

and shown in Fig. 11.1(b).

Downloaded from https://www.cambridge.org/core. UNIVERSIDAD AUTONOMA METROPOLITANA, on 19 Nov 2026 at 05:49:58, subject to the Cambridge Core terms of use, available at https://www.cambridge.org/core/terms. https://doi.org/10.1017/9781316219256.015

In Fig. 11.1(c) we compare the resulting Coulomb phase shift function with two others, both corresponding to unscreened charges. One of them represents a point charge (dashed, and "normalized" to coincide at the screening radius), the other to a distributed charge (solid). Outside of the positive charge ($b > R_+$), the two phase shift functions corresponding to an unscreened charge (point-like or distributed), are seen to only differ by a constant.

11.2 Screened Charge Distribution—Generalities

For a spherically symmetric charge distribution, one gets the familiar result for the phase shift function [11]

$$\chi_{\mathrm{C}}(b_x, b_y) = 4\pi\eta \left[\log b \int_0^b T_{\mathrm{C}}(b')b' \,\mathrm{d}b' + \int_b^\infty T_{\mathrm{C}}(b') \log b' b' \,\mathrm{d}b' \right], \tag{11.10}$$

where

$$b = \sqrt{b_x^2 + b_y^2}, \tag{11.11}$$

and where η is the Sommerfeld parameter,

$$\eta = \frac{Z_1 Z_2 \alpha}{\hbar v} \equiv \frac{Z_1 Z_2 e^2}{4\pi\hbar v}. \tag{11.12}$$

In Eq. (11.10), the logarithms do not refer to the scale of b. In fact, a scale R only contributes a constant amount $-2\eta \log(R)$ (compare Eq. (4.5)), which only modifies the scattering amplitude by an overall constant complex phase.

As seen previously, for cases with azimuthal symmetry, we need only the phase shift function evaluated in the scattering plane, i.e., for $b_y = 0$. Thus,

$$X_{\mathrm{C}}(b_x) \equiv \chi_{\mathrm{C}}(b_x, 0). \tag{11.13}$$

Up to an overall additive constant, as discussed above, one can thus write

$$X_{\mathrm{C}}(b_x) = 4\pi\eta \left[\log b_x \int_0^{b_x} T_{\mathrm{C}}(x) x \,\mathrm{d}x + \int_{b_x}^\infty T_{\mathrm{C}}(x) \log x \, x \,\mathrm{d}x \right], \quad \mathrm{Re}\, b_x > 0, \tag{11.14}$$

$$X_{\mathrm{C}}(-b_x) = X_{\mathrm{C}}(b_x). \tag{11.15}$$

For an arbitrary charge distribution, the stationary points will then be given in terms of $T_{\mathrm{C}}(b_x)$ as roots of either of the equations

$$X_{\mathrm{C}}{}'(b_x) = 4\pi\eta b_x^{-1} \int_0^{b_x} T_{\mathrm{C}}(x) x \,\mathrm{d}x = q, \quad \mathrm{Re}\, b_x > 0,$$

Downloaded from https://www.cambridge.org/core. UNIVERSIDAD AUTONOMA METROPOLITANA, on 19 Nov 2026 at 05:49:58, subject to the Cambridge Core terms of use, available at https://www.cambridge.org/core/terms. https://doi.org/10.1017/9781316219256.015

or

$$X_C'(b_x) = 4\pi\eta b_x^{-1}\int_0^{-b_x} T_C(x)x\,dx = q, \quad \mathrm{Re}\,b_x < 0. \tag{11.16}$$

If we consider next the second derivative,

$$X_C''(b_x) = 4\pi\eta b_x^{-1}\left[T_C(b_x)b_x - b_x^{-1}\int_0^{b_x} T_C(x)x\,dx\right], \quad \mathrm{Re}\,b_x > 0, \tag{11.17}$$

$$X_C''(-b_x) = X_C''(b_x), \tag{11.18}$$

we note immediately an important difference between the scattering from a point charge and that from a distributed charge. Whereas in the former case there is no rainbow point, there will in the latter case always be at least one rainbow singularity for a monotonically decreasing $T_C(b_x)$. It will occur at a value of the impact parameter $b_{x,R}$ for which the function $T_C(b_x)b_x$ is equal to its average over the interval from 0 to the points $b_{x,R}$,

$$T_C(b_{x,R})b_{x,R} = b_{x,R}^{-1}\int_0^{b_{x,R}} T_C(x)x\,dx. \tag{11.19}$$

This condition yields positive and negative solutions for $b_{x,R}$ which are equal in magnitude. Only one of the solutions, however, is consistent with the condition Eq. (11.16); it is the one for which X_C' is positive and $b_{x,R}$ has the same sign as η.

In contrast to the phase shift functions that we have encountered earlier, which were given in terms of some explicit, simple function, the present one is defined in terms of an integral along some non-trivial path in the complex b_x-plane. When the thickness function $T_C(b_x)$ has singularities in the complex b_x-plane, such integrals will depend on the path followed. We will return to this issue in Section 11.5.

11.3 A Simple Charge Distribution

As a particularly elementary example of an extended charge distribution, let us consider the one which generates the phase shift function

$$\chi_1(\boldsymbol{b}) = -C_\infty + 2\eta\log\sqrt{a^2+b^2}, \tag{11.20}$$

in which C_∞ represents a screening constant. (An overall scale in the argument of the logarithm has again been absorbed into C_∞.) We have chosen this expression as a simple analytic generalization of the Coulomb phase shift for a point charge. This phase shift function is easily shown via the solution to the Abel equation Eq. (2.6a) to correspond to a Coulomb potential

$$V_1(r) = \eta v\left[\frac{1}{a^2+r^2}\right]^{1/2}. \tag{11.21}$$

Downloaded from https://www.cambridge.org/core. UNIVERSIDAD AUTONOMA METROPOLITANA, on 19 Nov 2026 at 05:49:58, subject to the Cambridge Core terms of use, available at https://www.cambridge.org/core/terms. https://doi.org/10.1017/9781316219256.015

This potential corresponds to the charge density

$$\rho_1(r) = \frac{3a^2}{4\pi}\left[\frac{1}{a^2+r^2}\right]^{5/2}, \tag{11.22}$$

which has mean radius

$$\langle r\rangle = 2a. \tag{11.23}$$

The stationary impact parameters associated with the phase shift function Eq. (11.20) are given by the equation

$$X_1'(b_x) = 2\eta\frac{b_x}{a^2+b_x^2} = q, \tag{11.24}$$

which has only two solutions,

$$b_{jx} = \frac{\eta}{q} \pm \left[\left(\frac{\eta}{q}\right)^2 - a^2\right]^{1/2}. \tag{11.25}$$

These solutions are real inside the Coulomb rainbow point, $q < q_R$, with

$$q_R = \frac{\eta}{a}. \tag{11.26}$$

They are shown in Fig. 11.2 together with the cross section corresponding to $a = 3$ fm, for two different values of η, $\eta = 2$, and $\eta = 10$.

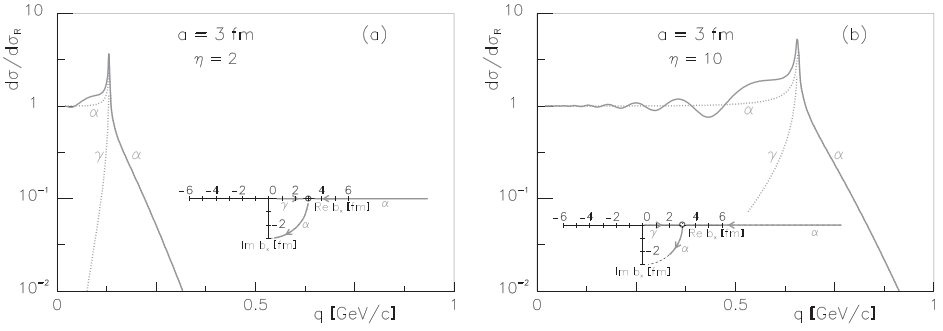


Figure 11.2 Differential cross section ratios $d\sigma/d\sigma_R$ for pure Coulomb scattering from the charge distribution $\rho_1(r) = (3a^2/4\pi)(a^2+r^2)^{-5/2}$, with $a = 3$ fm. Two values of the Sommerfeld parameter are considered, (a) $\eta = 2$, and (b) $\eta = 10$. The inserts show the trajectories of stationary points for $0.02\ \text{GeV/c} \le q \le 5.0\ \text{GeV/c}$ (dotted). The parts that correspond to the cross section plots, $0.02\ \text{GeV/c} \le q \le 1.0\ \text{GeV/c}$ are shown as solid curves. The open circles represent rainbow points. The cross section ratios contributed by the individual stationary points, α and γ, are shown as dotted curves. The solid curves give the resulting interference pattern, with the spikes representing rainbow singularities.

Downloaded from https://www.cambridge.org/core. UNIVERSIDAD AUTONOMA METROPOLITANA, on 19 Nov 2026 at 05:49:58, subject to the Cambridge Core terms of use, available at https://www.cambridge.org/core/terms. https://doi.org/10.1017/9781316219256.015

It is instructive to expand Eq. (11.25) inside the Coulomb rainbow point,[1]

$$b_{\alpha x} \simeq \frac{2\eta}{q}, \quad b_{\gamma x} \simeq \frac{\eta q}{2q_{\mathrm{R}}^2}; \quad q \ll q_{\mathrm{R}}. \tag{11.27}$$

The corresponding values of $X_1(b_{jx})$ and $X_1''(b_{jx})$ are approximately

$$X_1(b_{\alpha x}) \simeq 2\eta \log(2\eta/q); \quad X_1(b_{\gamma x}) \simeq 2\eta \log(\eta/q_{\mathrm{R}}); \tag{11.28}$$

$$X_1''(b_{\alpha x}) \simeq -\frac{q^2}{2\eta}; \qquad X_1''(b_{\gamma x}) \simeq \frac{2q_{\mathrm{R}}^2}{\eta}. \tag{11.29}$$

The two amplitudes may thus be approximated as

$$F(b_{\alpha x}) = -\frac{2ik\eta}{q^2} \exp\{2i\eta[-1 + \log(2\eta/q)]\}, \tag{11.30a}$$

$$F(b_{\gamma x}) = \frac{k\eta}{2q_{\mathrm{R}}^2} \exp\{2i\eta[-(q/2q_{\mathrm{R}})^2 + \log(\eta/q_{\mathrm{R}})]\}. \tag{11.30b}$$

For $q \ll q_{\mathrm{R}}$, $F(b_{\alpha x})$ will dominate $F(b_{\gamma x})$, and the familiar Rutherford cross section is obtained. But, as $q \to q_{\mathrm{R}}$, the interference term becomes increasingly important[2]

$$\begin{aligned}\left(\frac{\mathrm{d}\sigma}{\mathrm{d}q^2}\right)\Big/\left(\frac{\mathrm{d}\sigma}{\mathrm{d}q^2}\right)_{\mathcal{R}} &\simeq 1 + \frac{2\,\mathrm{Re}\,[F(b_{\alpha x})F^*(b_{\gamma x})]}{|F(b_{\alpha x})|^2} \\ &\simeq 1 - \frac{1}{2}\left(\frac{q}{q_{\mathrm{R}}}\right)^2 \sin\left\{2\eta\left[1 - \left(\frac{q}{2q_{\mathrm{R}}}\right)^2 + \log\left(\frac{q}{2q_{\mathrm{R}}}\right)\right]\right\},\end{aligned} \tag{11.31}$$

valid for $q \ll q_{\mathrm{R}}$.

We rewrite this as

$$1 - \frac{1}{2}\left(\frac{q}{q_{\mathrm{R}}}\right)^2 \sin[2\eta\phi(q)]. \tag{11.32}$$

The period of oscillation will be determined by

$$2\eta[\phi(q_{j+1}) - \phi(q_j)] = \pi, \tag{11.33}$$

or

$$\Delta q = q_{j+1} - q_j \simeq \frac{\pi}{2\eta}\left[\frac{\partial\phi}{\partial q}\right]^{-1}, \tag{11.34}$$

[1] Here, and in the next chapter, we shall denote the dominant stationary point by α, even though it (for Coulomb repulsion) occurs in the fourth quadrant.

[2] We emphasize that "$\mathcal{R}$" stands for "Rutherford," i.e., $(\mathrm{d}\sigma/\mathrm{d}q^2)_{\mathcal{R}} = (\mathrm{d}\sigma/\mathrm{d}q^2)_{\text{"Rutherford"}}$, while "R" means "Rainbow," $q_{\mathrm{R}} = q_{\text{"Rainbow"}}$.

Downloaded from https://www.cambridge.org/core. UNIVERSIDAD AUTONOMA METROPOLITANA, on 19 Nov 2026 at 05:49:58, subject to the Cambridge Core terms of use, available at https://www.cambridge.org/core/terms. https://doi.org/10.1017/9781316219256.015

where the index j labels the successive minima of the cross section ratio. By using

$$\frac{\partial \phi}{\partial q} = -\frac{q}{2q_{\mathrm{R}}^2} + \frac{1}{q}, \tag{11.35}$$

we obtain

$$\Delta q \simeq \frac{\pi}{2\eta} \frac{q\, q_{\mathrm{R}}^2}{q_{\mathrm{R}}^2 - \frac{1}{2}q^2}. \tag{11.36}$$

Within the present approximation, the period of oscillation thus increases with the momentum transfer, in an almost linear fashion. This behaviour is readily traced back to the phase of $F(b_{\alpha x})$, which depends on momentum transfer as $-2\eta \log(q)$. The oscillations are thus due to the rapid variation of the Coulomb phase.

The amplitude of the oscillation increases quadratically with q. This is a reflection of the q^{-2} behaviour of the "outer" Coulomb amplitude, $F(b_{\alpha x})$.

The cross sections given in Fig. 11.2 are based on the exact values for the stationary points.[3] The qualitative features of the cross section are seen to be consistent with those derived from the approximation, Eq. (11.27). In particular, the period of oscillation inside the rainbow for $\eta = 10$ changes with q in agreement with Eq. (11.36).

11.4 Gaussian Type Charge Distribution

We next consider a charge distribution which is somewhat less diffuse in nature. A simple such example, which leads to explicit analytic expressions for $\chi(\boldsymbol{b})$, is the generalized Gaussian charge distribution,

$$\rho_2(r) = \frac{1}{\pi^{3/2}\beta^3} \frac{1}{1+\frac{3}{2}\alpha} \left(1 + \alpha \frac{r^2}{\beta^2}\right) e^{-r^2/\beta^2}, \tag{11.37}$$

which is often encountered in shell models of the light nuclei. The corresponding Coulomb phase shift function is

$$\chi_2(\boldsymbol{b}) = -C'_\infty + 2\eta \left[\log\sqrt{b^2} + \frac{1}{2}E_1(b^2/\beta^2) + \frac{1}{2}\frac{\alpha}{1+\frac{3}{2}\alpha} e^{-b^2/\beta^2}\right], \tag{11.38}$$

where the exponential integral is defined as [2]

$$E_1(x) \equiv \int_x^\infty \frac{\mathrm{d}z}{z} e^{-z}. \tag{11.39}$$

[3] We do not here compare with the numerical evaluation of the diffraction integral. Because of the long range of the charge distribution, Eq. (11.22), these integrals cannot be evaluated without devising some special technique. A similar problem would of course be encountered if one tried to solve the Schrödinger equation for the potential $V_1(r)$, Eq. (11.21).

Downloaded from https://www.cambridge.org/core. UNIVERSIDAD AUTONOMA METROPOLITANA, on 19 Nov 2026 at 05:49:58, subject to the Cambridge Core terms of use, available at https://www.cambridge.org/core/terms. https://doi.org/10.1017/9781316219256.015

For $b_x = 0$, this gives

$$X_2(b_x) = -C'_\infty + 2\eta\left[\log(b_x) + \frac{1}{2}E_1(b_x^2/\beta^2) + \frac{1}{2}\frac{\alpha}{1+\frac{3}{2}\alpha}\, e^{-b_x^2/\beta^2}\right], \quad (11.40)$$

for $\mathrm{Re}\, b_x > 0$, and

$$X_2(-b_x) = X_2(b_x), \quad (11.41)$$

with

$$X'_2(b_x) = \frac{2\eta}{b_x}\left[1 - \left(1 + \frac{\alpha}{1+\frac{3}{2}\alpha}\,\frac{b_x^2}{\beta^2}\right)e^{-b_x^2/\beta^2}\right]. \quad (11.42)$$

The stationary point which constitutes a rainbow singularity can be found by solving

$$X''_2(b_x) = -\frac{2\eta}{b_x^2}\left\{1 - \left[1 + \frac{2}{1+\frac{3}{2}\alpha}\left(1 + \alpha + \alpha\,\frac{b_x^2}{\beta^2}\right)\frac{b_x^2}{\beta^2}\right]e^{-b_x^2/\beta^2}\right\} = 0, \quad (11.43)$$

provided $X'_2(b_x)$ is simultaneously real and positive. For $\alpha = 0$, the solution may be determined as $b_{x,\mathrm{R}} \simeq 1.121\beta$, and thus

$$q_\mathrm{R} = 1.276\frac{\eta}{\beta}; \quad (\alpha = 0). \quad (11.44)$$

The latter relation is qualitatively similar to Eq. (11.26). For a given geometry of the charge distribution, the rainbow value of $b_{x,\mathrm{R}}$ is again proportional to η and inversely proportional to the characteristic radius. As α increases from zero, the rainbow point moves slightly towards smaller momentum transfers.

In Fig. 11.3 we show the ratios of cross sections to the Rutherford cross section and (in the inserted graphs) the trajectories of the stationary points for $\chi_2(\boldsymbol{b})$ corresponding to two values of η ($\eta = 2$, and 10, in Fig. 11.3(a) and 11.3(b),

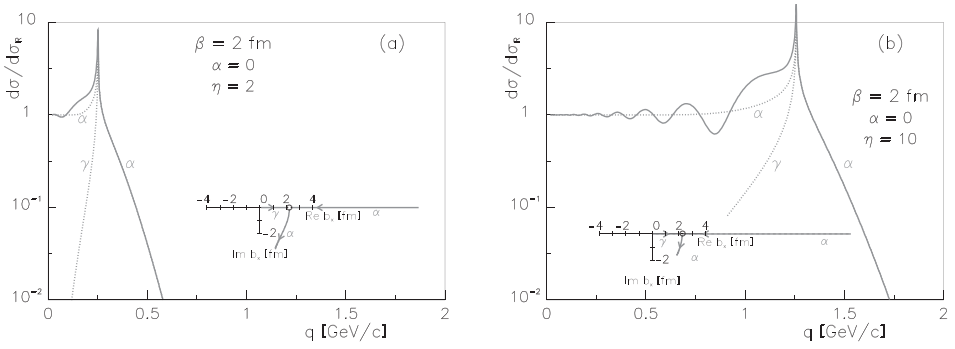


Figure 11.3 As Fig. 11.2, for the generalized Gaussian charge distribution of Eq. (11.37), with $\alpha = 0$ and $\beta = 2$ fm. Trajectories are shown for $0.02\ \mathrm{GeV/c} \leq q \leq 2.0\ \mathrm{GeV/c}$.

Downloaded from https://www.cambridge.org/core. UNIVERSIDAD AUTONOMA METROPOLITANA, on 19 Nov 2026 at 05:49:58, subject to the Cambridge Core terms of use, available at https://www.cambridge.org/core/terms. https://doi.org/10.1017/9781316219256.015

respectively), for $\beta = 2$ fm and $\alpha = 0$. The oscillations inside the rainbow point are similar to those found for $\chi_1(\boldsymbol{b})$ in Fig. 11.2. We see in particular, that for this case too, increase of η leads to an oscillating structure and a displacement of the rainbow point to a larger momentum transfer.

An interesting qualitative difference between these two phase shift functions appears outside the rainbow, for $q > q_{\mathrm{R}}$. Whereas the cross section corresponding to $\chi_1(\boldsymbol{b})$ is determined by only one stationary impact parameter, for $\chi_2(\boldsymbol{b})$ it is determined by two stationary impact parameters.

The stationary points $b_{\beta x}$ corresponding to $X_2(b_x)$ for $\alpha = 0$ are far from the real axis and thus not numerically important. However, for non-zero values of α they will move closer to the real axis. In this way, the phase shift function $\chi_2(\boldsymbol{b})$ may lead to cross section ratios that exhibit oscillations outside the rainbow point. This is illustrated in Fig. 11.4 for $\alpha = 2$. (The rainbow point for $\alpha = 2$ is given by $b_{x,\mathrm{R}} = 1.495\beta$ and $q_{\mathrm{R}} = 1.035\eta/\beta$.)

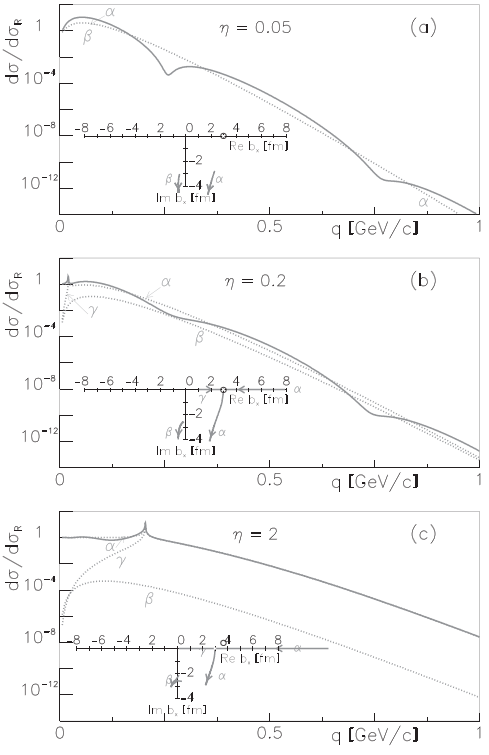


Figure 11.4 Differential cross section ratios $\mathrm{d}\sigma/\mathrm{d}\sigma_{\mathrm{R}}$ for pure Coulomb scattering from the generalized Gaussian charge distribution of Eq. (11.37), with $\alpha = 2$ and $\beta = 2$ fm. The figure illustrates how for this charge distribution oscillations are present outside the rainbow point for small values of η, but disappear when η becomes large. The trajectories of stationary points shown in the inserts correspond to the range of momentum transfer 0.01 GeV/c $\leq q \leq$ 1.0 GeV/c.

Downloaded from https://www.cambridge.org/core. UNIVERSIDAD AUTONOMA METROPOLITANA, on 19 Nov 2026 at 05:49:58, subject to the Cambridge Core terms of use, available at https://www.cambridge.org/core/terms. https://doi.org/10.1017/9781316219256.015

Figure 11.4 also illustrates an interesting dependence of the cross section ratio on the value of η. We see that when η is small, oscillations are present, whereas they gradually disappear as η increases. The reason for the disappearance of these oscillations is related to the relative values of the imaginary parts of the phase shifts, $\mathrm{Im}\, X_2(b_{j\,x})$. It turns out that $\mathrm{Im}\, X_2(b_{\alpha\,x})$ and $\mathrm{Im}\, X_2(b_{\beta\,x})$ are quite different in magnitude, and that difference increases rapidly with η. Since $F(b_{j\,x})$ contains, as a factor, $\exp[-\mathrm{Im}\, X_2(b_{j\,x})]$, it follows that when η becomes large, one of these amplitudes ($F(b_{\alpha\,x})$) will dominate the other one, ($F(b_{\beta\,x})$).

11.5 "Fermi" Type Charge Distribution

The third class of charge distributions we consider is the one that corresponds to the thickness function

$$T_{\mathrm{C}}(b) = T_0/\{1 + \exp[(b - c)/\beta]\}^p, \tag{11.45}$$

for $p = 1$ and 2. (The corresponding charge densities [see Eq. (11.7)] can be found by using the appropriate Abel equation.) In this case, the one-dimensional integrals [Eqs. (11.14)–(11.19)] that determine the phase shift function and its derivatives must be evaluated numerically. We denote the phase shift functions corresponding to the above thickness functions as $\chi_3(\boldsymbol{b})$ and $\chi_4(\boldsymbol{b})$, for $p = 1$ and 2, respectively. They are shown in Fig. 11.5 for real values of b_x. At large values, $b_x \gtrsim c$, they are very similar to each other, and to the point-charge phase shift function, $\chi_{\mathrm{pt}}(b_x)$.

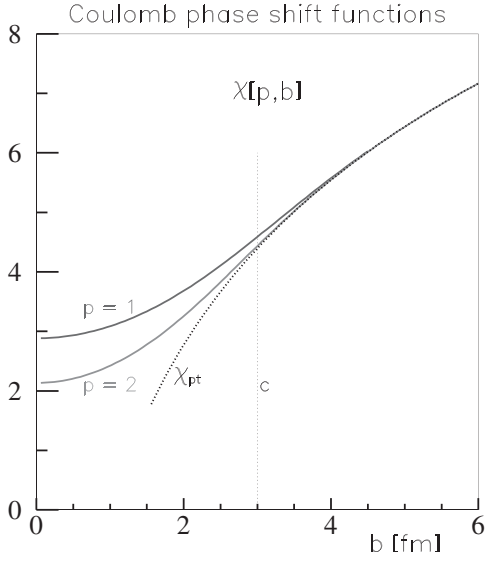


Figure 11.5 Phase shift function $\chi(b)$ corresponding to the thickness function (11.45), for $c = 3$ fm, $\beta = 0.5$ fm, $p = 1$, and $p = 2$. For reference, the phase shift function for a point charge is also shown.

Downloaded from https://www.cambridge.org/core. UNIVERSIDAD AUTONOMA METROPOLITANA, on 19 Nov 2026 at 05:49:58, subject to the Cambridge Core terms of use, available at https://www.cambridge.org/core/terms. https://doi.org/10.1017/9781316219256.015

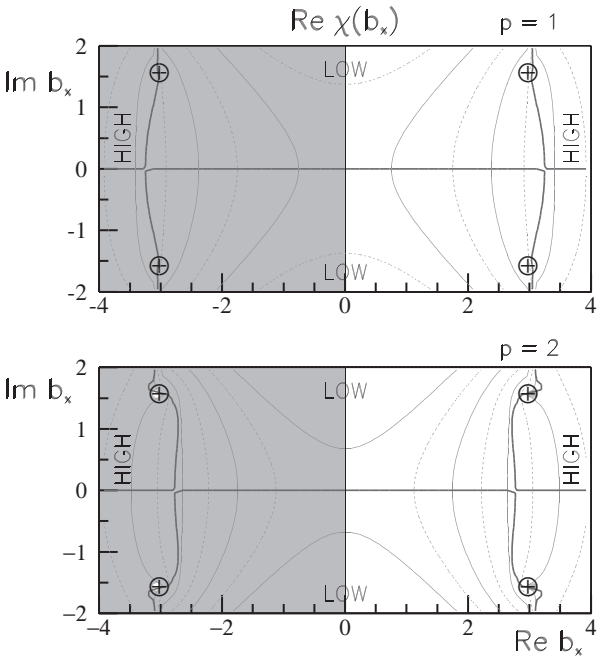


Figure 11.6 Phase shift function $\chi(b)$ corresponding to the thickness function (11.45), for $c = 3$ fm, $\beta = 0.5$ fm, $p = 1$, and $p = 2$, in the complex plane. Singular points at $b_x = \pm(c \pm i\pi\beta)$ are indicated, as well as lines along which $\mathrm{Im}\,\chi(b_x) = 0$ (heavy, dark). Stationary points are possible along these lines, if also $\mathrm{Re}\,\chi(b_x) = 0$ (white regions).

The phase shift functions $\chi_3(b_x)$ and $\chi_4(b_x)$ are explored in more detail in the complex b_x-plane in Fig. 11.6, where contours of constant $\mathrm{Re}\,\chi_3$ and $\mathrm{Re}\,\chi_4$ are shown.

Again, we see that at large values of $|\mathrm{Re}\,b_x|$, the two functions are rather similar. Moving away from the real axis, $\mathrm{Re}\,\chi(b_x)$ increases for $|\mathrm{Re}\,b_x| > c$, and decreases for $|\mathrm{Re}\,b_x| < c$. Actually, there are singularities at $b_x = \pm c + i\pi\beta$ and $b_x = \pm c - i\pi\beta$. Since the phase shift function is defined by an integral along a path in the complex b_x-plane, there will be lines of discontinuity attached to the singular points. These lines of discontinuous $\chi(b_x)$ have been taken parallel to the imaginary axis, away from the real axis.

Also indicated in Fig. 11.6, are regions where $\mathrm{Re}\,\chi'(b_x) > 0$ (white, possible regions of stationary phase points) and $\mathrm{Re}\,\chi'(b_x) < 0$ (dark). An important difference between the two cases is that for $p = 2$ (but not for $p = 1$), there are small regions in the left half-plane where $\mathrm{Re}\,\chi'(b_x) > 0$, indicated in white, close to the singularities $b_x = -c \pm i\pi\beta$. As we will see, the existence of these regions introduces an additional stationary point for $p = 2$.

Downloaded from https://www.cambridge.org/core. UNIVERSIDAD AUTONOMA METROPOLITANA, on 19 Nov 2026 at 05:49:58, subject to the Cambridge Core terms of use, available at https://www.cambridge.org/core/terms. https://doi.org/10.1017/9781316219256.015

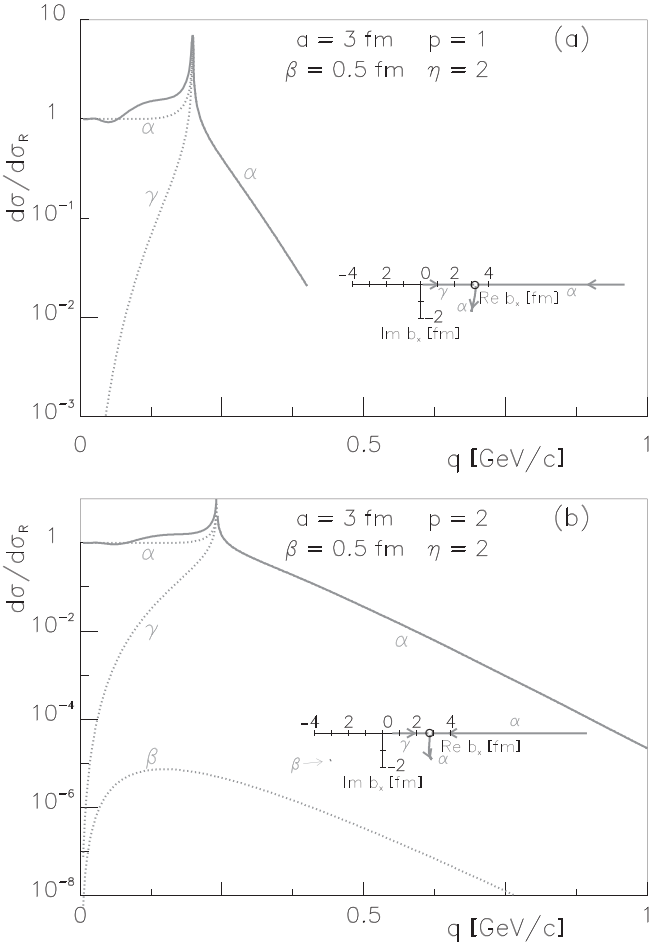


Figure 11.7 Differential cross section ratios $d\sigma/d\sigma_R$ for pure Coulomb scattering from charge distribution corresponding to the thickness function $T_C(b) = T_0/\{1+\exp[(b-c)/\beta]\}^p$, for $c = 3$ fm, $\beta = 2$ fm, and two values of the power p, (a) $p = 1$, and (b) $p = 2$. The strength of the interaction is in both cases the same, $\eta = 2$. As indicated by the inserts, for $p = 1$ there are only two trajectories, α and γ, and hence the differential cross section ratio falls smoothly outside the rainbow point. On the other hand, for $p = 2$, there is also a trajectory of stationary points, β, in the third quadrant, and outside the rainbow point the cross section ratio exhibits oscillations. The trajectories of stationary points shown in the inserts correspond to the range of momentum transfer 0.01 GeV/c $\leq q \leq$ 1.0 GeV/c.

The cross section ratios and the stationary point trajectories corresponding to X_3 and X_4 are shown in Fig. 11.7(a) and 11.7(b), respectively, for $c = 3$ fm, $\beta = 0.5$ fm, and $\eta = 2$. For $p = 1$ (Fig. 11.7(a)), there are two trajectories of stationary impact parameters, denoted $b_{\alpha x}$ and $b_{\gamma x}$, whereas for $p = 2$ (Fig. 11.7(b)), there are three, which we denote $b_{\alpha x}$, $b_{\beta x}$, and $b_{\gamma x}$. As a consequence, the cross

Downloaded from https://www.cambridge.org/core. UNIVERSIDAD AUTONOMA METROPOLITANA, on 19 Nov 2026 at 05:49:58, subject to the Cambridge Core terms of use, available at https://www.cambridge.org/core/terms. https://doi.org/10.1017/9781316219256.015

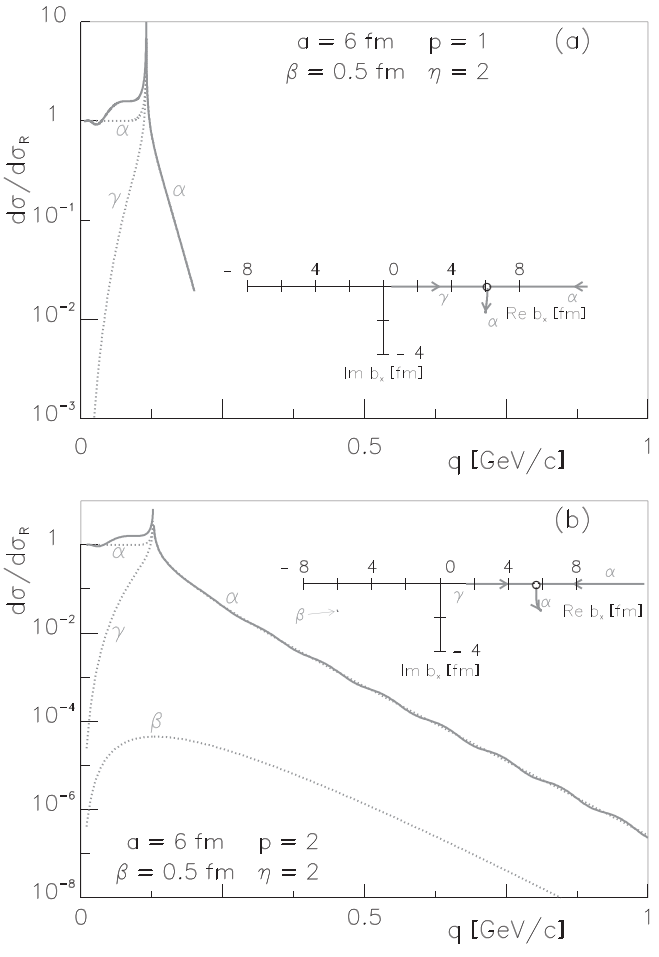


Figure 11.8 As Fig. 11.7, for $c = 6$ fm.

section for $p = 1$ has a smooth behaviour for $q > q_R$, whereas for $p = 2$ interference between $F(b_{\alpha x})$ and $F(b_{\beta x})$ leads to an asymptotically regular oscillatory pattern in the differential cross section, with a period inversely proportional to c. This behaviour is shown in Fig. 11.8, where the corresponding plots have been given for a radius twice as large, $c = 6$ fm.

One interesting property of the phase shift function X_4 ($p = 2$) is that the trajectory of stationary points $b_{\beta x}$ is limited to a very small neighborhood of the singularity, located at $b_x = -c - i\pi\beta$. Also, in contrast to what we found for the Gaussian charge distribution [$\chi_2(\boldsymbol{b})$, with $\alpha \neq 0$], the oscillations of the cross section ratios remain strong, even for large values of η. This behaviour is related to the fact that the stationary points are closer to the real axis, so that $\mathrm{Im}\, X(b_{\alpha x})$ and $\mathrm{Im}\, X(b_{\beta x})$ are less different in magnitude.

Downloaded from https://www.cambridge.org/core. UNIVERSIDAD AUTONOMA METROPOLITANA, on 19 Nov 2026 at 05:49:58, subject to the Cambridge Core terms of use, available at https://www.cambridge.org/core/terms. https://doi.org/10.1017/9781316219256.015

A general comment can be made here concerning the existence of the trajectory of stationary points, $b_{\beta x}$. Let us suppose the thickness function has a singularity of the type

$$T(b) = T_{\mathrm{R}}(b - b')^{-\nu} + \text{L.S.T.}, \tag{11.46}$$

where "L.S.T." is meant to indicate "less singular terms." The stationary points will then be given asymptotically for large q by

$$\epsilon\left[4\pi\eta\frac{T_{\mathrm{R}}}{1-\nu}(b_{jx} - b'_x)^{-(\nu-1)} + \text{L.S.T.}\right] = q, \quad \text{for } \nu \neq 1, \tag{11.47}$$

and

$$\epsilon\big[4\pi\eta T_{\mathrm{R}} \log(b_{jx} - b'_x) + \text{L.S.T.}\big] = q, \quad \text{for } \nu = 1, \tag{11.48}$$

where

$$\epsilon = \mathrm{Re}\,(b_{jx})/|\,\mathrm{Re}\,(b_{jx})|. \tag{11.49}$$

We can assume without loss of generality that $\eta > 0$. Changing the sign of η simply interchanges the roles of the stationary points α and β.

A simple analysis then shows that Eq. (11.47) will have solutions $b_{\beta x}$ [$\mathrm{Re}\,(b_{\beta x}) < 0$] as well as $b_{\alpha x}$ [$\mathrm{Re}\,(b_{\alpha x}) > 0$], provided $\nu > 3/2$. On the other hand, for $\nu \leq 3/2$, the solution $b_{\beta x}$ does not exist. This is indeed the case for $X_3(b_x)$. It may be noted that the above argument breaks down if the singularity is integrable, i.e., for $\nu < 1$. These results are summarized in Table 11.1.

Our study of Coulomb scattering from extended charge distributions can be summarized as follows: Inside the rainbow point the cross section ratios exhibit oscillations due to the interference of amplitudes contributed by trajectories $b_{\alpha x}$ and $b_{\gamma x}$. The crucial feature leading to these characteristic oscillations is the fact that the secondary amplitude, $F(b_{\gamma x})$, has a phase that varies slowly compared to that of the dominant, "outer" Coulomb amplitude, $F(b_{\alpha x})$. Due to the infinite tail of the Coulomb potential, the rate of change of the phase of $F(b_{\alpha x})$ is, for small q, approximately $2\eta/q$.

Table 11.1 *Existence of $b_{\beta x}$ for $T(b) = T_R(b-b')^{-\nu}+$L.S.T.*

Range in ν	Existence of $b_{\beta x}$
$\nu < 1$	No statement
$1 \leq \nu \leq \frac{3}{2}$	$b_{\beta x}$ does not exist
$\frac{3}{2} < \nu$	$b_{\beta x}$ exists

Downloaded from https://www.cambridge.org/core. UNIVERSIDAD AUTONOMA METROPOLITANA, on 19 Nov 2026 at 05:49:58, subject to the Cambridge Core terms of use , available at https://www.cambridge.org/core/terms. https://doi.org/10.1017/9781316219256.015

This may be contrasted with the corresponding rate of change of the amplitudes resulting from the short-range real phase shift functions which were studied in Chapters 7 and 8. For example, for the real Gaussian phase shift function, the rate of change of the phase $-qb_{\alpha x} + X(b_{\alpha x})$ behaves for small q roughly as $\sqrt{\log q}$, as can be seen from Eq. (7.8). In the next chapter we shall see that, as combinations of Coulomb and strong interactions are considered, similar patterns will arise. However, in such cases, the most important among the secondary amplitudes may as well be associated with the nuclear interactions as with the charge distribution (as was the case here).

For $q > q_{\mathrm{R}}$, on the other hand, the cross section may or may not show oscillations, depending on the existence and location of the trajectory $b_{\beta x}$.

Patterns similar to some of those shown in this chapter are observed in electron–nucleus scattering [5], where the asymptotic approach may also be of use. Electron scattering differs from hadron scattering, however, in two important aspects:

- Spin effects are important at large momentum transfers.
- At moderate energies, noneikonal effects, i.e., corrections to elementary diffraction theory are important. These may be accounted for by adding a suitable $1/k$-correction term to the phase shift function.

Downloaded from https://www.cambridge.org/core. UNIVERSIDAD AUTONOMA METROPOLITANA, on 19 Nov 2026 at 05:49:58, subject to the Cambridge Core terms of use , available at https://www.cambridge.org/core/terms. https://doi.org/10.1017/9781316219256.015